Reduction of Nitric Acid to Hydroxylamine at Glassy Carbon Surfaces Modified by the Reduction of *p*-Phenylenediamine and *p*-Aminophenol in 1.0 M Nitric Acid

A Scanning Electrochemical Microscopy Study

Lara I. Halaoui,[a] Hossein Sharifian,[b,*] and Allen J. Bard[a,**]

[a]*Department of Chemistry and Biochemistry, The University of Texas at Austin, Austin, Texas 78712, USA*
[b]*SACHEM, Incorporated, Austin, Texas 78704, USA*

The scanning electrochemical microscope (SECM) was used to study the electrochemical reduction of nitric acid to hydroxylamine at modified glassy carbon (GC) electrodes. The GC surface was modified by holding it at a negative potential in solutions of *p*-aminophenol, or *p*-phenylenediamine in 1.0 M nitric acid. The generated products were detected in generation/collection experiments with an SECM Pt ultramicroelectrode. The films that form on GC, apparently polymers of a quinone imine intermediate, can also be grown under similar conditions on indium tin oxide (ITO) coated glass electrodes and appeared as dark orange-brown films. Atomic force microscope imaging revealed a highly porous structure. SECM and cyclic voltammetry studies showed that as a result of this surface filming, the GC electrodes exhibited an increase of at least 1 V in the hydrogen overpotential relative to the unmodified surface and the efficiency of the electrochemical reduction of nitric acid to hydroxylamine was dramatically enhanced. Bulk electrolysis of nitric acid at carbon in the presence of *p*-phenylenediamine resulted in a 75 to 85% current efficiency for hydroxylamine production at current densities of 0.5 to 0.8 A/cm^2. This procedure proved to be useful for the large-scale electrochemical production of hydroxylamine from nitric acid at an electrode other than liquid mercury.
© 2001 The Electrochemical Society. [DOI: 10.1149/1.1389343] All rights reserved.

We report here a modification of a carbon electrode surface that greatly increases the hydrogen overpotential in nitric acid solutions and allows electrochemical generation of hydroxylamine with a good current efficiency. Hydroxylamine was first discovered by Lossen, and reported in 1868.[1] In the agricultural and pharmaceutical industries, it serves as an intermediate for various synthetic end products. The semiconductor industry benefits from its use in stripper formulations for photoresist removal. It also finds applications as a component in liquid propellants, as a reducing agent, and as a photographic developer. Interest in the synthesis of hydroxylamine from nitric acid reduction and an understanding of the mechanism leading to its formation thus stems from its value in many chemical industries and the complexity of the reduction processes often used in its synthesis.

One major synthetic process for hydroxylamine is the hydrogenation of HNO$_3$ on a catalytic surface,[2] where HNO$_3$ is catalytically hydrogenated to nitrous acid, which is then reduced to hydroxylamine and ammonia. The electrochemical reduction of nitric acid, nitrous acid, and their salts was proposed using amalgamated lead electrodes by Tafel in 1902.[3] Electrochemically, the reduction of nitric acid to hydroxylamine only occurs efficiently with Hg or amalgam electrodes via the reaction[4]

$$NO_3^- + 8H^+ + 6e \rightarrow H_3NOH^+ + 2H_2O \qquad [1]$$

With most other electrodes, the evolution of hydrogen occurs at or before nitrate reduction or the materials are unstable in the nitric acid environment. An additional problem is the possible further reduction of the hydroxylamine at the electrode to ammonia

$$NO_3^- + 10H^+ + 8e \rightarrow NH_4^+ + 3H_2O \qquad [2]$$

In this work, we address the need to find a safe, inexpensive, and environmentally friendly electrode material to replace mercury for the electrolytic synthesis of hydroxylamine, a goal thus far unattained. We describe a novel surface modification of a carbon electrode and the formation of a film that inhibits proton reduction but promotes nitrate reduction to hydroxylamine.

The scanning electrochemical microscope (SECM) was used to study the electrochemical reduction of HNO$_3$ on glassy carbon (GC) electrodes modified under reducing potentials in solutions of *p*-aminophenol or *p*-phenylenediamine in 1 M HNO$_3$. SECM allowed the detection at a Pt ultramicroelectrode of electroactive species produced at the substrate. SECM results showed this modification procedure, which generated a film on carbon and indium tin oxide (ITO) surfaces, to result in a dramatic increase in the efficiency of nitric acid reduction to hydroxylamine at GC and a decrease in hydrogen evolution at all potentials. Cyclic voltammetric studies also revealed an increase in the overpotential of proton reduction to hydrogen at GC as a result of this surface filming. The presence of nitric acid was shown to be important in film growth. Atomic force microscopy (AFM) and scanning electron microscopy (SEM) images were used to address the film morphology. Possible mechanisms for the effect of such surface modification in promoting this reduction process are discussed. The grown films are believed to promote this process by providing a catalytic surface for nitrate reduction while inhibiting proton reduction to hydrogen gas.

Experimental

Chemicals.—Hydroxylamine was a 50% wt/vol aqueous solution (SACHEM Inc., Austin, TX); a stabilizer had been added to prevent decomposition. For bulk electrolysis and generation/collection experiments, *p*-phenylenediamine (PPD) (Aldrich) was used without recrystallization. In cyclic voltammetry (CV) experiments performed to study the effect of electrode filming on hydrogen evolution, PPD crystals of 99+% purity (Aldrich) were utilized. The *p*-aminophenol (PAP) (Aldrich) was in the form of pure white crystals 98+%. Acid solutions, 1.0 M, were prepared by diluting nitric acid (EM, 69-71%), perchloric acid (MEB, 71%), or hydrochloric acid (EM, 36.5-38%). All solutions were made using deionized (DI) water (Millipore, resistivity ≥18 MΩ cm).

Electrodes.—Triply distilled Hg (Bethlehem Apparatus Co., Inc.) was used as substrate for SECM experiments. ITO coated glass (Delta Technologies) was cleaned by sonication in DI water and ethanol in an ultrasonic cleaning bath for at least 5 min in each solvent, prior to being mounted as electrodes. A 10 μm diameter Pt tip sealed in glass (CH Instruments, Austin, TX) was used as the ultramicroelectrode in this work. GC disks of 2 or 3 mm diam were mounted in Teflon, and served as working electrodes or as SECM

substrates. Pt wires were heated and sealed in glass to form 2 mm diam disk electrodes. When first mounted, working electrodes were polished to a mirror finish with 0.1, 0.3, and 0.05 μm alumina. Before each subsequent use, the electrodes were further polished with 0.05 μm alumina. For surface cleaning subsequent to modification, the GC electrodes were slightly sanded on Carbimet paper (600 grit, Buehler), then polished to a mirror finish with 0.3 and 0.05 μm alumina. Before all experiments, the potential of the GC electrodes was cycled between -0.2 and -2.0 V in 1.0 M nitric acid, to ensure their surfaces had restored the hydrogen evolution characteristics of the unmodified surface.

A Pt wire (Aldrich) or graphite felt [Shunk GFS8(1/2 in.)] served as an auxiliary electrode for the SECM setup. For other electrochemical work, Pt gauze (Aldrich) or graphite felt was employed. To eliminate the possibility of Pt dissolution in nitric acid and subsequent deposition on the cathodic working electrode with Pt auxiliary electrodes, a carbon felt auxiliary electrode was also used. The nature of the auxiliary electrode material did not affect the results of this work. All potentials are reported *vs.* Ag/AgCl reference electrodes assembled using 3 mm diam porous Vycor rods sealed in heat-shrinkable Teflon tubing (BAS, West Lafayette, IN).

Instrumentation.—CV was carried out with a model 660 electrochemical workstation (CH Instruments). Generation/collection experiments were performed with a commercial SECM (CH Instruments).

Surface modification.—Electrochemical measurements were performed in three-electrode glass cells. Solutions were deaerated with nitrogen for 20 min, with a nitrogen blanket maintained over the solution. Concentrations of 5 to 6 mM PPD or PAP solutions in 1.0 M nitric, perchloric, or a mixture of the acids were used for GC modification. The potential of the GC electrode was cycled between -0.1 and -2.0 V at 100 mV/s or 1.0 V/s. A potential positive of -0.1 V was never applied to the GC electrodes in these experiments (neither before modifying their surfaces nor when measuring the onset of hydrogen evolution at the unmodified surface). Accordingly, both the electrochemical oxidation of the carbon surface and filming due to electrochemical oxidation of PAP or PPD were avoided. ITO electrodes (3 cm^2) were treated in 50 mM PAP or PPD in 1.0 M nitric acid or perchloric acid by cycling their potential between -0.1 and -2.0 V at 100 mV/s. To form thick films that could be peeled off the ITO surfaces, the potential was cycled 50 to 80 times.

SECM experiments.—SECM experiments were performed in Teflon cells exposed to the atmosphere, in a four-electrode configuration with two working (substrate and tip), auxiliary, and reference electrodes. In all cases, anodic currents are taken as negative. For adjusting the tip-to-substrate approach, oxygen reduction at the Pt tip was used and the distance determined from the negative feedback response. After the initial coarse approach, the Pt tip was activated by cycling its potential between proton reduction and water oxidation (-0.4 and 2.3 V, respectively), at a rate of 500 mV/s, until the oxygen reduction wave was distinguished. Subsequently, the Pt tip was held at 0.2 to 0.3 V, a potential suitable for oxygen reduction at Pt.

Before each measurement of HNO$_3$ reduction, the Pt tip was activated (for hydroxylamine detection) by cycling its potential 10 times between -0.4 and 2.3 V at 500 mV/s (with the GC substrate potential maintained at -0.1 or -0.2 V and the Pt substrate at -0.1 V). After the tip surface activation step, the substrate was held at the specified negative potential and the tip potential was scanned at 50 mV/s, with the tip current in the resulting voltammogram used to detect products generated at the substrate.

In studying the effect of carbon surface modification, the HNO$_3$ solution was replaced with 5 mM solutions PPD or PAP in 1.0 M HNO$_3$. The GC electrode was held at negative potentials (-0.9 to -1.2 V) or cycled in the region -0.2 to -2.0 V in these solutions. The cell was then flushed with 1.0 M HNO$_3$, without displacing the

tip. Similar to the case of the unmodified surface, the substrate was held at the specified negative potential in 1.0 M HNO$_3$, and the tip current was measured as its potential was scanned at 50 mV/s to detect generated products.

Bulk electrolysis.—The electrolysis cell (plate and frame) consisted of titanium coated with ruthenium dioxide as the anode (25 cm^2), a graphite and carbon felt cathode (25 cm^2), and a Nafion 423 cation selective membrane as the cell divider. High surface area graphite felt GFS8 (1/2 in.) obtained from Shunk (area to volume ratio: 1.0 m^2/35 cm^3) was pressed against the graphite to increase the active surface area of the cathode. A piece of polypropylene mesh was placed between the membrane and the graphite felt to prevent the membrane from touching the felt. In a typical electrolysis, a solution of 50 mM PPD in 1.0 M HNO$_3$ was added to the cathode half-cell, and a 4.0 M HNO$_3$ solution was added to the anode half-cell. The catholyte and anolyte solutions were circulated into the compartments at a flow rate of 0.40 gal/min. Nitric acid was periodically introduced with a metering pump into the cathode half-cell to keep the molarity between 0.25 and 0.5 M. The cell temperature was maintained between 10 and 15°C.

AFM and SEM imaging.—Films of PAP for AFM imaging were grown on freshly exposed planes of highly oriented pyrolytic graphite (HOPG) mounted as electrodes, from 50 mM PAP in 1.0 M HNO$_3$ by cycling the potential between -0.2 and -2.0 V at 100 mV/s (50-60 cycles). For SEM imaging, films of PAP were grown on ITO-glass electrodes using the same procedure and solution described above (80 cycles). The films were washed with DI water (by multiple slow dipping in DI water so as not to disturb the adhesion on the surface), and allowed to air dry before imaging. AFM imaging was carried out under ambient conditions with a Nanoscope III (Digital Instruments) microscope. A silicon nitride cantilever tip (Digital Instruments) was used. SEM imaging was conducted using an E3 Electroscan environmental scanning electron microscope. The chamber was pressurized at 5 Torr with water vapor, after being pumped down to 1 Torr; the energy of the electron beam was at 25 V.

Results and Discussion

Electrochemical detection of hydroxylamine.—The electrochemical detection of hydroxylamine in 1.0 M HNO$_3$ was possible via monitoring its oxidation at a Pt tip ultramicroelectrode. To obtain a well-defined wave for hydroxylamine oxidation, it was necessary to carry out a potential cycling pretreatment of the Pt surface. The oxidation of hydroxylamine occurs via a complex mechanism, involving various byproducts and intermediates depending on the electrode and the electrolyte.[5] Surfaces other than Pt, *e.g.*, Au and graphite are less suitable than Pt for this oxidation, perhaps because of the catalytic effect of Pt on the decomposition of hydroxylamine. Various values are reported for the number of electrons, *n*, involved in this half reaction. Lingane and Jones reported $n = 2.7$ for the coulometric oxidation of hydroxylammonium chloride in NaCl supporting electrolyte at Pt.[6] Davis[7] studied this oxidation at Pt at pH 1-13, with chronopotentiometry and found $n = 6$, while coulometry yielded $n = 2$ to 4.6; the *n* value decreased with increasing acidity. The discrepancies of results between the two methods were attributed to differences in the effects of the Pt oxide film. This oxidation was kinetically more facile at a finely divided reduced Pt surface than at an oxide covered one.[8] A factor of 6.6 increase in the current for hydroxylamine oxidation in 1.0 M sulfuric acid resulted from using a platinized rotating Pt electrode as opposed to an untreated surface.[5] We found it necessary to carefully pretreat the Pt tip in the 1.0 M HNO$_3$ medium used in this work to obtain reliable analytical results.

Figure 1A, curve a, shows a background scan at the 10 μm Pt tip ultramicroelectrode in 1.0 M HNO$_3$, showing the onset of background oxidation current at 1.15 V, and a reduction peak at 0.55 V, revealing the formation and reduction of an oxidized Pt surface.
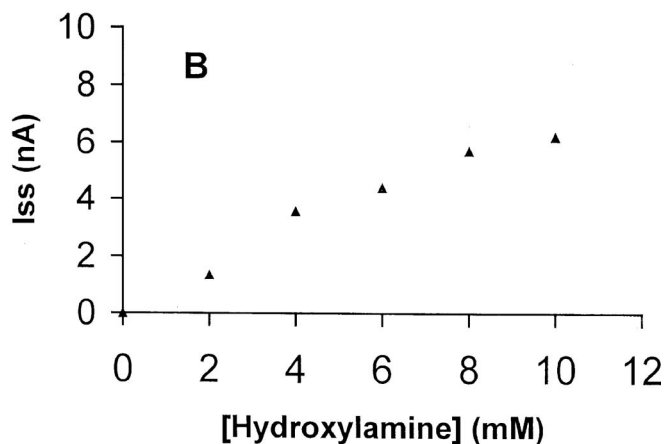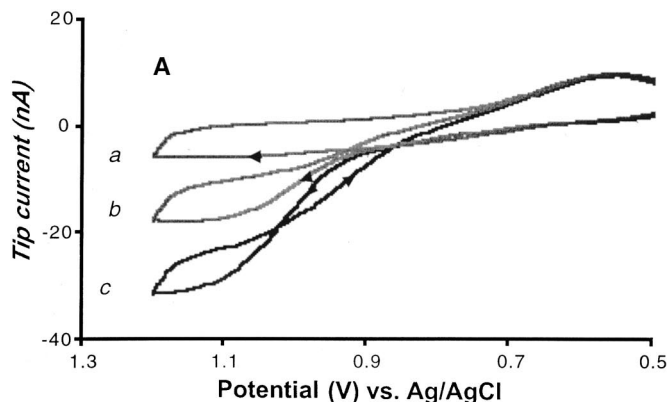
Figure 1. (A) Cyclic voltammograms at a 10 μm Pt tip ultramicroelectrode of (a) 0, (b) 20, and (c) 55 mM hydroxylamine in 1.0 M HNO_3; scan rate is 50 mV/s. (B) Plot of the steady-state current measured at 1.15 V after background subtraction at different hydroxylamine concentrations between 2 and 10 mM.

Figure 2. SECM with Hg substrate in 1.0 M HNO_3: Plot of tip current at 1.15 V as a function of the potential of the Hg substrate. The tip current was measured from the corresponding cyclic voltammograms acquired at 50 mV/s scan rate.

Curves b and c show CVs at the same electrode in 20 and 55 mM solutions of hydroxylamine in 1.0 M HNO_3. These CVs were acquired after the potential of the Pt electrode was cycled between oxygen and hydrogen evolution (−0.4 and 2.3 V) to create a freshly reduced Pt surface. This electrode pretreatment was necessary for the hydroxylamine electrochemical oxidation to be reproducible and for the steady state current measured at 1.15 V to show a linear dependence on the concentration between 2 and 10 mM (and in fact to concentrations to 55 mM) (Fig. 1B).

In 1.0 M HNO_3, the electrochemical oxidation of hydroxylamine at Pt thus occurs at potentials positive of 0.9 V, with a limiting current in the potential region between 1.1 and 1.2 V. The smaller oxidation current seen on the reverse scan probably results from some oxidation of the Pt electrode surface, which decreases the rate of hydroxylamine oxidation. The electrochemical oxidation of Pt and hydroxylamine occurs in the same potential region, as is apparent from the background oxidation current of 6 nA at 1.15 V (Fig. 1A, curve a). Another important feature appears in the CV of 55 mM hydroxylamine (Fig. 1A, curve c), where the oxidation current on the reverse sweep is larger than that on the forward scan, starting at 1.0 V. This kind of hysteresis is generally diagnostic of surface effects, in this case the reduction of Pt surface oxide by the relatively high concentration of hydroxylamine, thus changing the nature of the surface during the scan.

SECM study of nitric acid reduction.—SECM was used to study the reduction of HNO_3 at GC, Pt, and Hg substrates, by scanning the SECM tip in the region of potentials where hydroxylamine could be detected. The Pt tip was positioned over the substrate at a known
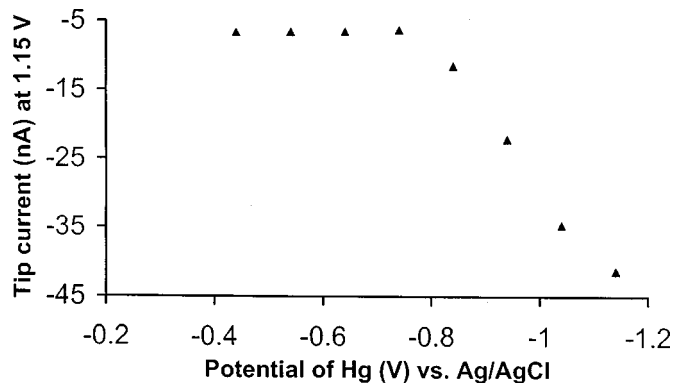
distance by determining the approach curve for oxygen reduction at the tip and fitting the results to that of an insulating substrate. The Pt tip was held in close proximity (5 to 10 μm separation distance) from the substrate surface. The substrates were then held at various potentials and the products of HNO_3 reduction were detected. Hydroxylamine produced from the reduction of HNO_3 was detected at the SECM Pt tip by measuring the oxidation current at 1.15 V. The use of SECM for generation/collection experiments dramatically reduces the experimental time needed for each measurement and allows ready determination of the yield of hydroxylamine as a function of potential, electrode material, and surface treatment and solution conditions.

The success of this measurement depends on the lack of oxidation of dissolved hydrogen at the Pt tip when it is held at a potential where it is covered by an oxide film. As shown in a previous SECM study of Pt tip collection of dissolved hydrogen produced at a Pt cathode,[9] oxide film formation on Pt suppresses hydrogen oxidation in acidic solution. Thus, at a potential of 1.15 V, any hydrogen generated at the substrate will not be detected at the Pt tip.

In a first experiment, to demonstrate the feasibility of hydroxylamine detection above a cathode, Hg was employed as the generating cathode, since it is known to give a high yield of product. The tip oxidation current at 1.15 V was measured with the tip in close proximity to the Hg surface from cyclic voltammograms acquired while the substrate was held at the specified potential. Figure 2 shows such oxidation current as a function of the substrate potential. Starting at a potential of −0.7 V at the Hg substrate, HNO_3 reduction results in hydroxylamine production.

We then studied the reduction of HNO_3 at a newly polished GC substrate and with PAP or PPD modified GC surfaces. In cases where the GC surface was modified, the HNO_3 solution was replaced by 5 mM PAP or PPD solutions, both 1.0 M in HNO_3 without changing the tip-GC distance. This was done to ensure that the reduction was studied under the same conditions of tip-sample separation with the modified and clean carbon surfaces. This method was employed because the O_2 reduction current at the Pt tip, monitored to control the tip approach, decreased with time possibly due to surface inactivation and could differ in experiments with and without PAP or PPD. The only constraint on the reproducibility of the tip-substrate separation distance with the solution replacement protocol was possible small thermal or vibrational effects.

When the potential of the unmodified GC substrate was held between −0.1 and −0.4 V (*e.g.*, Fig. 3A), the oxidation current at 1.15 V at the Pt tip was similar in magnitude to the background current (measured with the tip far away from the substrate). This indicated the absence of reduction of HNO_3 to hydroxylamine at these potentials. When the GC substrate was held at −0.5 V or more negative potentials (*e.g.*, Fig. 3B), no significant wave at 1.15 V was
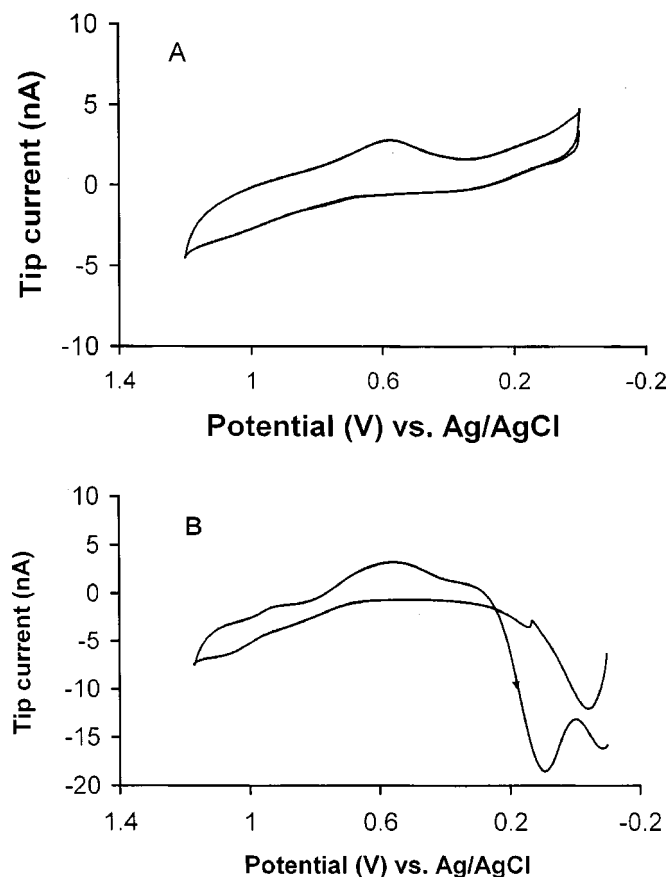
Figure 3. SECM with a GC substrate in 1.0 M HNO_3: CVs at a 10 μm Pt tip ultramicroelectrode obtained with the substrate held at (A) −0.2, and (B) −0.5 V.

Figure 4. SECM with a Pt substrate in 1.0 M HNO_3: CV at a 10 μm Pt tip ultramicroelectrode obtained with a Pt substrate held at −0.22 V.

Figure 5. SECM with PAP modified GC surface in 1.0 M HNO_3: CVs at a 10 μm Pt tip ultramicroelectrode, with the modified substrate held at (a) −0.2, (b) −0.6, (c) −0.8, and (d) −1.0 V; 50 mV/s scan rate.

seen, but a significant oxidation current was measured between −0.2 and 0.5 V. This current decreased when the potential was driven more positive. This can probably be attributed to the production of H_2 gas at the GC substrate. SECM results on the reduction of nitric acid at a Pt substrate showed a similar behavior. This is depicted in Fig. 4, where a Pt substrate was held at −0.22 V. Holding the potential of this substrate at −0.1 V resulted in a cyclic voltammogram at the Pt tip identical to the background scan (similar to that in Fig. 1A, curve a). At Pt substrate potentials negative of −0.2 V,
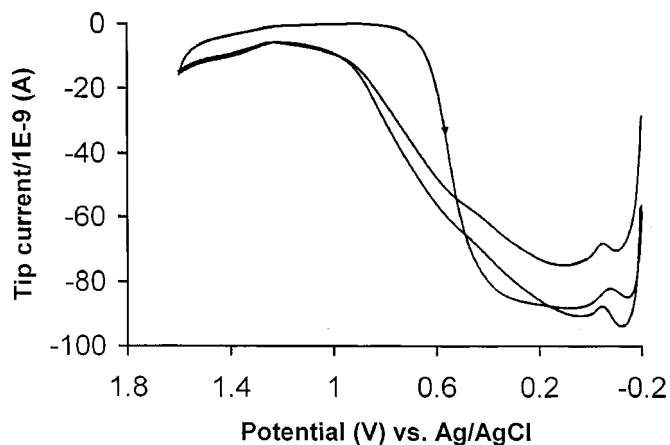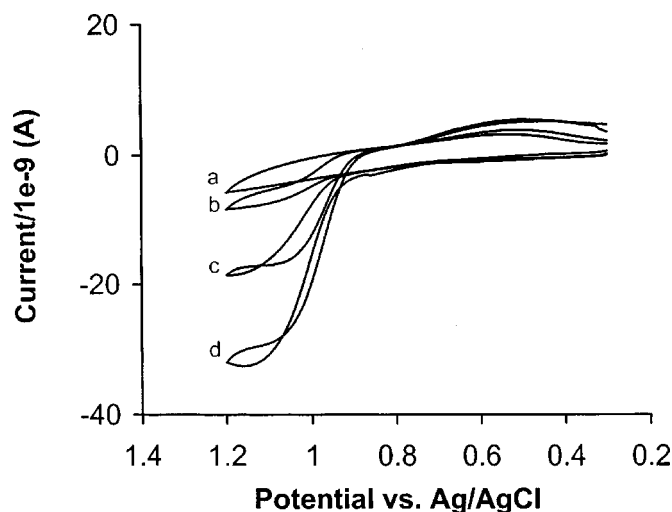
where hydrogen evolution takes place, a significant oxidation current is measured at the Pt tip. This current decreased as the potential was scanned positive, again demonstrating the absence of interference from hydrogen in the range of tip potentials where hydroxylamine oxidation is measured. Thus in 1.0 M HNO_3, protons are reduced to hydrogen gas at potentials negative of −0.2 V at Pt and at −0.5 V at GC surfaces. The tip oxidation currents starting at −0.2 V and decaying away as the potential is scanned positive correspond to the oxidation at the Pt tip of hydrogen gas evolved at the GC or Pt surfaces. The previous SECM study of hydrogen detection at a Pt tip[9] was carried out in $HClO_4$ solution where the tip surface conditions at potentials in the H_2 oxidation region remained quite stable. However, some chemical oxidation of the Pt tip takes place in 1 M HNO_3 that inactivates it with time toward hydrogen oxidation. This oxidation explains the dramatic decrease in tip current to only slightly more than the background current at anodic potentials as the Pt becomes oxidized. It also explains the increase in oxidation current on the reverse scan at potentials where the oxidized Pt surface is reduced (about 0.55 V), and hence, reactivated toward hydrogen oxidation by the presence of a freshly reduced Pt surface.

SECM results on the reduction of 1 M HNO_3 at GC modified with PAP or PPD showed a significant increase in hydroxylamine yield. Figure 5 shows SECM results in 1 M HNO_3 with a PAP-modified GC substrate. The substrate had been previously cycled between −0.2 and −1.6 V in 5 mM PAP in 1.0 M HNO_3 at 100 mV/s. The PAP-modified GC surface was held at −0.2, −0.6, −0.8, and −1.0 V, after the above solution was replaced with 1 M HNO_3. Oxidation currents of 18 and 32.4 nA were measured at a 1.15 V tip potential, when the modified substrate was held at −0.8 and −1.0 V, respectively (Fig. 5, c and d). The corresponding background current was 4.9 nA with the substrate held at −0.2 V (Fig. 5, a). The hydroxylamine oxidation current at a 1.15 V tip potential after background subtraction (substrate at −0.2 V) is plotted in Fig. 6 as a function of the potential of the PAP-modified GC surface. The oxidation current increased as the substrate potential was driven to more negative values until it reached a maximum at −1.0 V. This maximum could be attributed to a competing process of proton reduction, which becomes more significant at more negative potentials after surface modification. At potentials where hydroxylamine is produced at this substrate (negative of −0.6 V), the corresponding oxidation current was considerably larger than that measured for the untreated GC surface, and hydrogen oxidation at the tip considerably smaller.
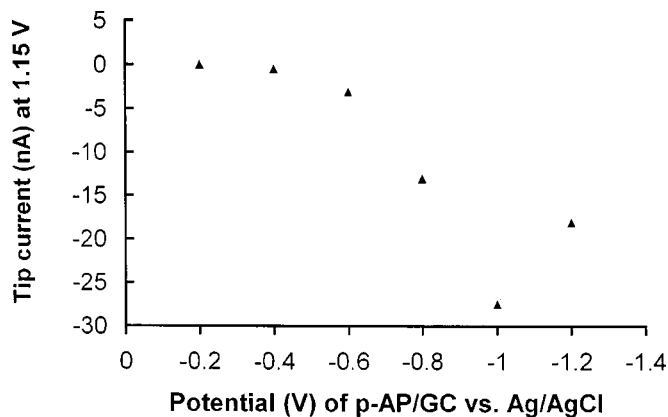
Figure 6. SECM with PAP modified GC surface in 1.0 M HNO_3: Plot of the oxidation current measured at 1.15 V tip potential as a function of the PAP-modified GC potential. The tip current was measured from the corresponding cyclic voltammograms acquired at 50 mV/s scan rate.

A hydrogen oxidation current as large as 120 nA was measured at a tip potential of 0.35 V, with an anodic current of 12 nA at 1.15 V, with the unmodified GC substrate held at −1.15 V. The background current in this case was between 7 and 8.5 nA, with the substrate held at −0.25 V. Upon holding the PAP-modified GC at −1.15 V, the hydrogen oxidation current at the tip (at 0.35 V) decreased to 6 nA. On the other hand, an oxidation current of 36 nA resulting from hydroxylamine oxidation was seen at a 1.15 V tip potential. Thus, at least a fivefold increase in hydroxylamine oxidation current resulted from this surface modification (assuming perhaps a small contribution from hydrogen oxidation in the measurement, especially at the unmodified surface). Two consequences are thus shown to result from this surface modification of the GC: (*i*) hydrogen gas is not detected at the tip while the PAP-modified GC surface is held at potentials negative of −0.5 V, and (*ii*) HNO_3 is reduced to hydroxylamine at this surface as indicated by this latter oxidation at tip potentials positive of 0.9 V. The surface treatment thus suppresses hydrogen evolution on the GC and permits HNO_3 reduction to hydroxylamine.

The same effects were observed upon modifying the GC surface, at negative potential, in solutions of PPD/1.0 M HNO_3. In addition to increasing the yield of hydroxylamine, changing the carbon surface with PPD dramatically reduced hydrogen gas evolution. The oxidation current at 1.15 V tip potential is plotted after background subtraction before and after PPD modification (Fig. 7). For the data shown in Fig. 7, b, the substrate potential was scanned between −0.1 and −1.2 V in 5 mM PPD/1.0 M HNO_3.

CV study of the effect of surface modification on proton reduction.—Figure 8, a, shows a typical cyclic voltammogram in 1.0 M HNO_3 at a GC electrode, showing the onset of proton reduction at −0.5 V (note that only H_2 was detected with SECM at this potential). Figure 8, b, shows the first scan in 5.6 mM PAP/1.0 M HNO_3 at 100 mV/s, between −0.1 and −1.2 V. A decrease in the current occurred when the potential was scanned negative of −0.8 V in the presence of PAP. Further potential cycling in this region resulted in a continuous decrease in the reduction current, until a maximum cathodic onset potential for hydrogen evolution was reached. Figure 8, c, shows a cyclic voltammogram measured after 10 scans in the same solution, between −0.1 and −1.2 V at 100 mV/s. About a 1.2 V increase in the hydrogen overpotential (taken arbitrarily at 20 mA) resulted from this surface treatment. After this treatment, cycling the potential of the PAP-modified GC surface 85 times, between −0.1 and −1.5 V at 100 mV/s, in 1.0 M HNO_3 (not containing PAP) did not restore the original hydrogen overpotential. The
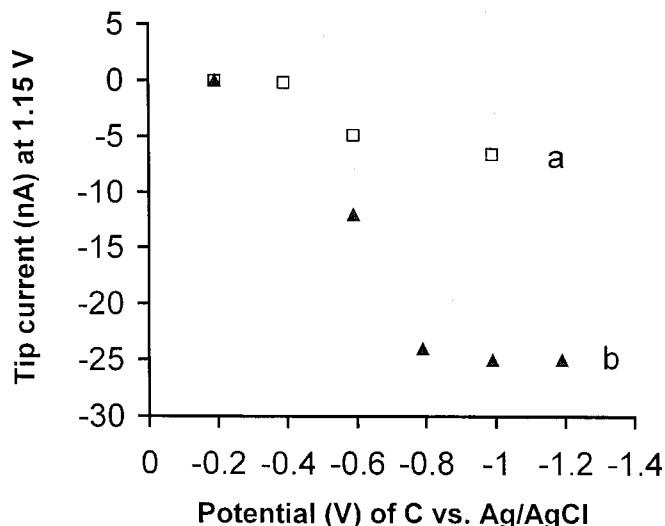

Figure 7. Oxidation current measured at 1.15 V at the SECM Pt tip as a function of the potential of the GC substrate (a) unmodified, and (b) modified with PPD in 1.0 M HNO_3. The tip current is measured from the corresponding cyclic voltammograms at 50 mV/s scan rate.

characteristic potential onset at −0.5 V in 1.0 M HNO_3 was restored only after the surface was mechanically polished and cycled in HNO_3.

The same effect on the hydrogen overpotential was observed for PPD-modified GC surfaces as a result of surface modification. The current-voltage (I-V) plot in Fig. 9, a, is again typical behavior of a GC electrode in 1.0 M HNO_3; the difference from Fig. 8, a, is possibly due to slight differences in the surface active sites for proton reduction. The first scan in 5 mM PPD/1.0 M HNO_3 (Fig. 9, b) between −0.1 and −1.2 V at 100 mV/s showed a decrease in the current, similar to the one observed for PAP. After applying 12 cycles (between −0.1 and −2.0 V at 100 mV/s), a 1.1 V increase in the hydrogen evolution onset was measured (Fig. 9, c).

Evidence for film formation.—ITO electrodes provided a large surface area (3 cm^2) for film growth and permitted an examination of the film. To form thick films, the ITO electrode potential was cycled between −0.1 and −2.0 V at 100 mV/s in 50 mM PAP or PPD in 1.0 M HNO_3. As grown on ITO, these films appeared as
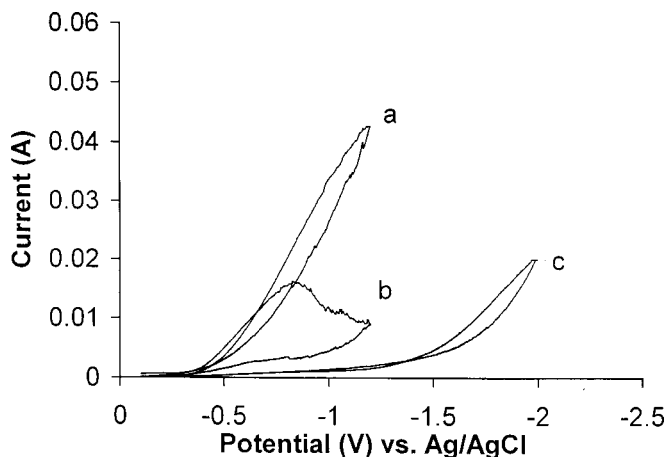

Figure 8. CVs at GC electrode in 1.0 M HNO_3 (a) first scan in 5.6 mM PAP/1.0 M HNO_3 solution (b) after 10 scans between −0.1 and −1.2 V in 5.6 mM PAP/1 M HNO_3 (c) scan rate, 100 mV/s. (Scanning the potential between −0.1 and −2.0 V gives similar result and was sometimes used).
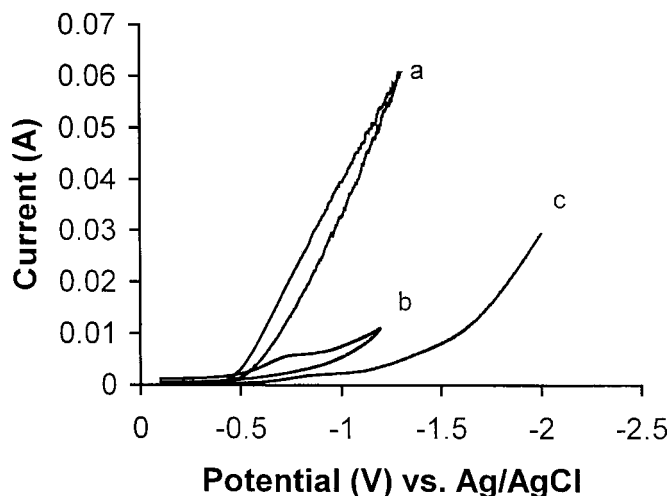
Figure 9. CVs at GC electrode in 1.0 M HNO_3 (a), first scan in 5.0 mM PPD/1.0 M HNO_3 solution (b), after 12 scans in this latter solution between -0.1 and -2.0 V (c); scan rate, 100 mV/s.

dark orange-brown material that could be peeled off the electrode surface while wet. Treatment of ITO using the same cycling procedure in 50 mM PAP in 1.0 M perchloric acid showed no film formation on the surface. SEM and AFM imaging was used to examine film morphology. SEM images of PAP-modified ITO glass did not reveal the presence of defects or holes in the film aside from the observed cracks believed to result from film drying on the underlying ITO surface in the vacuum environment. AFM imaging at higher resolution of PAP-modified HOPG, on the other hand, revealed a grainy film morphology. Figure 10A corresponds to an AFM image (5×5 μm) of a clean HOPG surface, with a flat morphology characteristic of this material. Figure 10B shows an AFM image at 1×1 μm of a PAP film on HOPG. The particle-like nature of film growth gave rise to pores of 50-100 nm in width, measured from AFM cross sections.

Dependence of surface modification on the presence of nitric acid.—Surface modification involving filming of the electrode surface depended on the specific presence of nitric acid. Attempts to grow these films in perchloric and hydrochloric acids were unsuccessful. Filming of the electrode surface was noted in 1.0 M perchloric acid only after a small amount of nitric acid was added.

Figure 11 shows the onset of hydrogen evolution at GC in 1.0 M nitric, perchloric, and hydrochloric acids. The overpotential for this process showed a dependence on the medium. Hydrogen evolution started at -1.2 V in 1.0 M HCl, at -1.0 V in 1.0 M $HClO_4$, and at -0.5 V in 1.0 M HNO_3. A reasonable explanation is that formation of oxidized sites on the surface promotes the reduction of protons. Reactions on carbon electrodes are known to be very sensitive to the surface treatment.[10]

Cycling the GC electrode between -0.2 and -2.0 V at 1.0 V/s and 100 mV/s in 5 mM PAP/1.0 M perchloric acid solutions did not result in filming of the electrode surface. However, if a small amount of nitric acid (20 mM) was added, filming occurred. These experiments were performed according to the following procedure. CV on a clean GC surface was acquired in 1.0 M HNO_3 to test the absence of any previous surface films. The electrode was then thoroughly rinsed with DI water and transferred into a 1.0 M $HClO_4$ solution where a cyclic voltammogram was taken, and the onset of proton reduction measured. The potential of the electrode surface was then cycled in the PAP/specified acid solution in a procedure similar to the one in HNO_3. The electrode was tested for any shift in proton reduction onset potential in the same medium. The electrode was then taken out of the solution and returned to 1.0 M HNO_3,
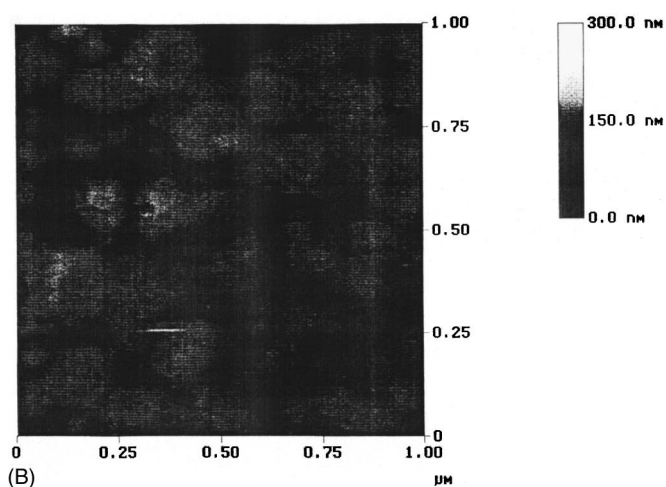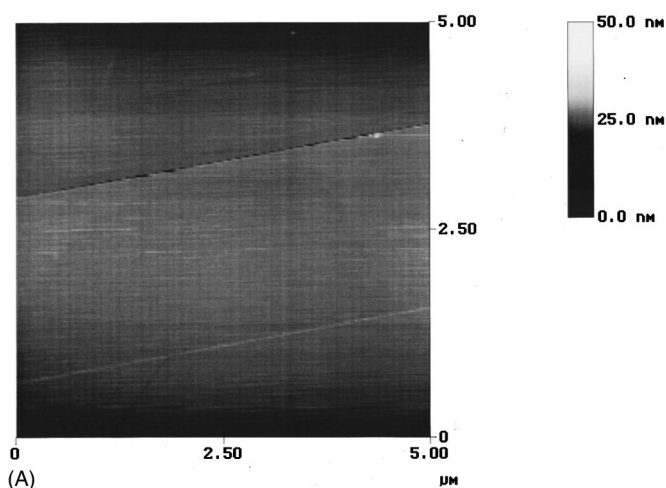

Figure 10. AFM images. (A) untreated HOPG; (B) typical film prepared with PAP.

where a cyclic voltammogram was taken. Figure 12 shows the I-V characteristics of a GC electrode in 1.0 M HNO_3, after this surface has been treated in (a) 5 mM PAP/1.0 M perchloric acid in the absence of nitric acid, and (b) in the presence of 20 mM nitric acid. Before electrode treatment in the absence of nitrate, the onset of H_2
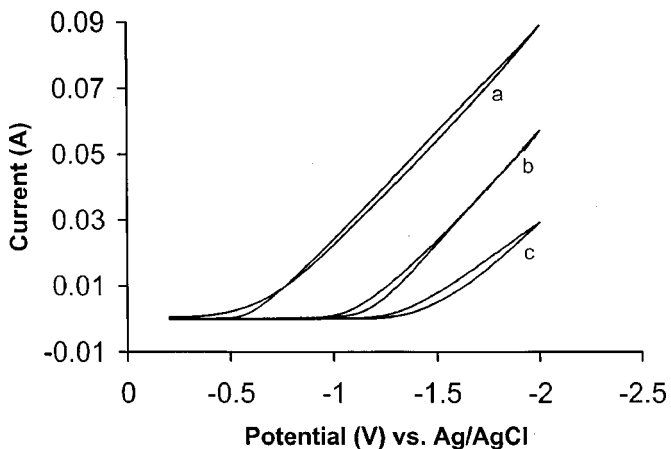

Figure 11. Cyclic voltammograms at GC in 1 M HNO_3 (a), perchloric acid (b), and hydrochloric acid (c). Scan rate, 1 V/s.
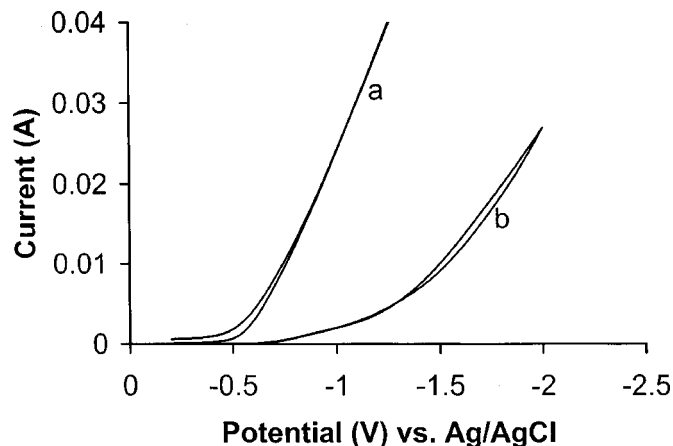
Figure 12. Cyclic voltammograms at GC in 1.0 M HNO_3 after the electrode surface had been treated with 5 mM PAP in 1.0 M perchloric acid (a), and with 5 mM PAP in 1.0 M perchloric acid after addition of 20 mM HNO_3 (b).

evolution in 1.0 M HNO_3 occurred at -0.5 V, characteristic of an unmodified GC surface. On the other hand, a 0.9 V increase in the hydrogen overpotential resulted from surface modification.

Effect of film on other electrode reactions.—The increase of the hydrogen overpotential with a filmed GC electrode was smaller for other media than in HNO_3. For example for 0.5 M KOH, the increase was about 0.3 V, while for 0.5 M KCl, it was about 0.35 V. Although the film allowed reduction of HNO_3 and production of hydroxylamine, it was blocking for other electrode reactions. For example, the reduction of ferricyanide in 0.5 M KCl was blocked by the film.

Nature of the film.—The growth of a polymeric film on the electrode occurs by the reduction of PAP or PPD in 1 M HNO_3. While there have been numerous studies of the oxidation of PAP and PPD,[11] the reduction of these species has not been studied. A polymer of PPD surfaces has been shown to grow only under oxidizing potentials. Polymer formation by a cathodic process from PAP and PPD has not been previously reported. The films formed in HNO_3 upon reduction of PAP and PPD, appear yellow-brown to the naked eye and have been imaged by SEM as grown on ITO, and by optical microscopy on GC, and by AFM on HOPG. However, their molecular structure has not been identified. With high resolution imaging by AFM, they appear to be grainy on the hundred nanometer scale with some porosity and a relatively smooth surface (50-100 nm corrugations) (Fig. 10). There may be interconnected pores into the depth of the films that can provide pathways for ion migration.

The presence of HNO_3 was needed for film growth. This suggests that a first chemical oxidation of PAP by HNO_3 is involved in the formation of an intermediate, perhaps the quinone imine (QI), that is reduced to form the film. The PAP and PPD molecules are related through a following oxidation/reduction process. CV of PPD in 1.0 M nitric acid revealed the presence of an irreversible oxidation with $E_{1/2}$ at 0.9 V, followed by a reversible redox process with $E_{1/2} = 0.6$ V, similar to the behavior reported by Adams *et al.* of PPD in 1.0 M perchloric acid.[12] CV of PAP in this medium showed a reversible pair of waves with $E_{1/2} = 0.6$ V. PPD undergoes a two-electron oxidation in acidic media to the diimine. The radical cation of PPD, detected by electron spin resonance under less acidic conditions, had not been detected in strong acids, according to reported work by Adams *et al.*[12,13] The diimine hydrolyzes to the quaternary tetraalkylammonium iodide (QI) in strong acids; this latter is reduced reversibly to PAP, resulting in the redox process at 0.6 V. Thus one can speculate that oxidation of PPD by HNO_3 to PAP, followed by further oxidation by HNO_3 to the QI occurs. The reduction of QI would then produce the polymer. Further mechanistic studies are needed to verify this mechanism and obtain better structural data for the film.

What is especially intriguing is how this film increases the hydrogen overpotential so strongly in HNO_3. Perhaps it prevents oxidation and activation of the carbon surface, making the behavior closer to that found in nonoxidizing acids, like HCl. Carbon surface effects are known to be very important in the kinetics of heterogeneous electron transfer, *e.g.*, during the formation of new functionalities (*e.g.*, OH, COOH, CO).[10] The film does not prevent reduction of HNO_3 to hydroxylamine however, so, in the absence of hydrogen evolution, the current efficiency increases dramatically.

It is also possible that the film changes the nature of adsorption sites on the carbon. For example, if the film prevented adsorption of proton, but allowed (or promoted) adsorption of nitrate ion, this would favor hydroxylamine formation.[4] The electrochemical reduction of HNO_3 is believed to involve an adsorbed species. Germanium dioxide deposited as germanium on Pt in 1.25 M sulfuric acid and catalyzing nitrate reduction has been reported to cause a significant decrease in the hydrogen adsorption peak at Pt and an increase in the HNO_3 reduction peak.[14,15] Germanium was reported to promote HNO_3 adsorption and to inhibit hydrogen adsorption. The reduction of HNO_3 on the Ge/Pt surface was said to involve adsorbed hydrogen, so that a high amount of Ge was found to inhibit the reduction of HNO_3 to nitrite by blocking all of the adsorption sites available for atomic hydrogen. Further evidence for the involvement of adsorbed species comes from the suppressing effect of different adsorbing ions on the reduction rate of HNO_3. This was again attributed to competitive adsorption between the studied electrolytes and nitric acid.[16,17]

Bulk electrolysis results.—Electrolysis was carried out in an electrochemical flow cell as described in the experimental section. Typical results are given in Table I. Further details are available.[18]

Conclusions

Reduction of solutions of PAP or PPD in 1.0 M HNO_3 at GC resulted in surface modification by filming of the electrode surfaces.

Table I. Bulk electrolysis results.

Catholyte[a]	Additive	Current density (A/cm^2)	Cell voltage (V)	Product HAN (M)	Residual HNO_3 (M)	Current efficiency (%)
1 M HNO_3	50 mM PPD	0.05	4.0	1.3	0.8	60
1 M HNO_3	50 mM PPD	0.47	5.0	1.7	0.6	75
0.5 M HNO_3	50 mM PPD	0.78	6.5	1.67	0.5	85
0.5 M HNO_3	0[b]	0.78	6.0	1.35	0.6	70
0.5 M HNO_3	70 ppm PAP	0.78	6.5	1.26	0.7	74

[a] The solution was maintained at 0.5 to 1 M HNO_3 during electrolysis by additions of HNO_3.
[b] Cathode filmed in the preceding experiment was employed.

This filming takes place on ITO electrodes as well, and, in all cases, requires the presence of HNO_3. The modified GC electrodes showed an increase in the hydrogen overpotential of 1.1 to 1.2 V, relative to unmodified ones. This modification was shown by SECM to allow the reduction of HNO_3 to hydroxylamine on GC with good efficiency because of the decreased hydrogen evolution. Bulk electrolysis measurements showed up to 75-85% current efficiency for hydroxylamine production with a product specificity favoring hydroxylamine as final product, without significant further two-electron reduction of hydroxylamine to ammonia.

References

1. W. Lossen, *Annalen. Suppl.,* **6**, 220 (1868).
2. (a) W. C. Bull, H. C. Zeisig, P. D. Strickler, and E. G. Marhofer, U.K. Pat. 772,670 (1953); (b) A. H. de Rooy, U.K. Pat. 1,094,221 (1967).
3. J. Z. Tafel, *Anorg. Chem.,* **31**, 289 (1902).
4. R. L. Dotson, *Electrochem. Soc. Interface*, **3**, 35 (1994).
5. S. S. Lord, Jr. and L. B. Rogers, *Anal. Chem.,* **26**(3), 284 (1954).
6. J. I. Lingane and S. L. Iones, *Anal. Chem.,* **23**, 1804 (1951).
7. D. J. Davis, *Anal. Chem.,* **35**, 764 (1963).
8. G. R. Rao and L. Meites, *J. Phys. Chem.,* **70**, 3620 (1966).
9. J. Zhou, Y. Zu, and A. J. Bard, *J. Electroanal. Chem.,* **491**, 22 (2000).
10. R. L. McCreey, in *Electroanalytical Chemistry*, Vol. 17, A. J. Bard, Editor, p. 221, Marcel Dekker, New York (1966).
11. See, *e.g.*, (a) R. C. Reed and R. M. Wightman, in *Encyclopedia of the Electrochemistry of the Elements*, Vol. 15, Chap. 1, A. J. Bard, Editor, Marcel Dekker, New York (1984); (b) R. N. Adams, *Electrochemistry at Solid Electrodes*, p. 327, Marcel Dekker, New York (1969).
12. Z. Galus, H. Y. Lee, and R. N. Adams, *J. Electroanal. Chem.,* **5**, 17 (1963), and references therein.
13. H. Y. Lee and R. N. Adams, *Anal. Chem.,* **34**, 1587 (1962).
14. G. R. Rao and L. Meites, *J. Phys. Chem.,* **70**, 3620 (1966).
15. J. F. van der Plas and E. Barendrecht, *Electrochim. Acta,* **25**, 1463 (1980).
16. G. Horanyi and E. M. Rizmayer, *J. Electrochem. Chem.,* **140**, 347 (1982).
17. M. Wasberg and G. Horanyi, *Electrochim. Acta,* **40**, 615 (1995).
18. H. Sharifian and H. Wagonknecht, U.S. Pat. 6,024,855 (2000).